Fluorescence Anisotropy of Nile Red and Oxazine 725 in an Isotropic Liquid Crystal

Myungjin Choi, Daeseong Jin, and Hackjin Kim*

Department of Chemistry, College of Natural Sciences, Chungnam National University, Taejon 305-764, Korea

Tai Jong Kang

Department of Chemistry, College of Natural Sciences, Taegu University, Kyungsan 712-714, Korea

Sae Chae Jeoung and Dongho Kim

Spectroscopy Laboratory, Korea Research Institute of Standards and Science, Taejon 305-600, Korea

Received: April 2, 1997; In Final Form: August 10, 1997[⊗]

Steady-state and time-resolved fluorescence anisotropy for nile red and oxazine 725 in the isotropic phase of the liquid crystal *p*-methoxybenzylidene-*n*-butylaniline (MBBA) are measured in the temperature range 50−80 °C. The fluorescence characteristics of the dye molecules in the isotropic MBBA agree well with the Perrin equation over the investigated temperature range. The decay of the fluorescence anisotropy of the dye molecules in the isotropic liquid crystal follows the simple hydrodynamic (Debye−Stokes−Einstein) model rather than the Landau−de Gennes model for the orientational dynamics of neat isotropic liquid crystals. These results imply that the microscopic anisotropy, which is important in the dynamics of neat isotropic liquid crystals, has no effects on the reorientation dynamics of the dopant dye molecules. Attractive interactions among MBBA molecules are so strong that the dopant molecules are not embedded in the pseudonematic domains of the isotropic phase. The dielectric friction affects the reorientation dynamics to give small deviations from the simple hydrodynamic model.

Introduction

Fluorescence anisotropy is one of the various spectroscopic techniques employed for the study of the reorientation dynamics of probe molecules and the structure and solvation dynamics of liquid phases.[1−11] The fluorescence anisotropy $r(t)$ is defined by

$$r(t) = [I_{||}(t) - I_{\perp}(t)]/[I_{||}(t) + 2I_{\perp}(t)] \quad (1)$$

where $I_{||}(t)$ and $I_{\perp}(t)$ are the fluorescence intensities parallel and perpendicular to the polarization of the excitation light. Generally the fluorescence anisotropy decays exponentially as the molecules excited by the polarized light lose the anisotropy by rotation. The reorientation dynamics are usually interpreted in terms of the hydrodynamic model[12] where the solute molecule is assumed to undergo rotation in a continuous medium. The reorientation time, τ, corresponding to the fluorescence anisotropy decay time, is usually given by the Debye−Stokes−Einstein (DSE) equation in the hydrodynamic model

$$\tau_{DSE} = \eta V f/kT \quad (2)$$

where η is the viscosity of the medium, V is the van der Waals volume of the rotating molecule, f is the molecular shape factor, k is the Boltzmann constant, and T is the temperature. The DSE equation is modified depending on the boundary conditions (stick vs slip).[13] In addition to the hydrodynamic friction, there exists dielectric friction for the polar molecules in nonpolar medium.[1−5,11,14,15]

The reorientation dynamics deviate from the DSE equation when the probe molecule isomerizes in the excited state[6,7] or the local environment for the probe molecule is quite different from what is deduced from the bulk properties of the solution.[8,9,16] For liquid crystals, anisotropic intermolecular interactions are retained well above the nematic−isotropic transition temperature (T_{NI}).[17] Local structures of the isotropic liquid crystal, called pseudonematic domains, make the isotropic liquid crystals distinct from normal liquids. The pseudonematic domains, considered as small nematic droplets, undergo uncorrelated dynamic motions, and the domain size is usually referred by the coherence or correlation length on the order of several to a few tens of molecular lengths. The rotation of the isotropic liquid crystal molecule is strongly coupled with the motions of the pseudonematic domain. On the basis of mean field theory, de Gennes suggested the modified hydrodynamic model (Landau−de Gennes (LdG) model) for the rotation of the isotropic liquid crystal. According to the LdG model, the orientational time of the isotropic liquid crystal molecule, τ_{LdG}, is expressed by

$$\tau_{LdG} = \eta V/k(T - T^*)^{\gamma} \quad (3)$$

where T^* is a temperature slightly below T_{NI}, γ is a constant around one, and the other parameters are the same as in eq 2.

The orientational dynamics of the liquid crystal molecules in the isotropic phase studied by the transient grating optical Kerr effect method have been reported.[18,19] The temperature-independent fast dynamics and the slow dynamics obeying the LdG model were observed for the neat isotropic liquid crystals. The slower process was attributed to the randomization of the pseudonematic domains and the faster one displaying a power law decay to the intradomain dynamics. If dopant molecules were strongly coupled with the liquid crystal molecules, the orientational time of the dopant molecule would be much larger in the isotropic liquid crystal than in normal liquids of the same viscosity and temperature as seen from the comparison of eqs 2 and 3.

[⊗] Abstract published in *Advance ACS Abstracts,* September 15, 1997.

S1089-5647(97)01157-7 CCC: $14.00

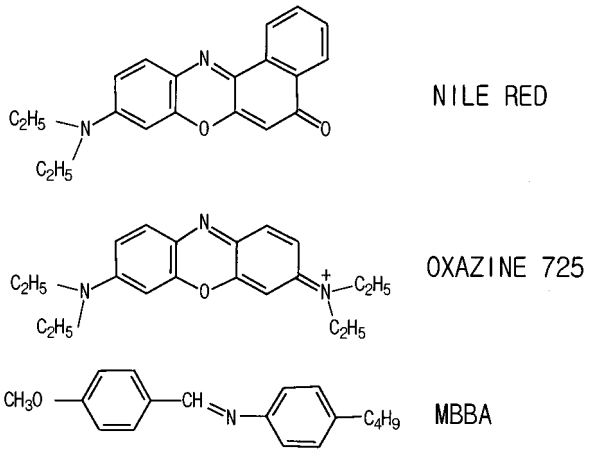

Figure 1. Molecular structures of nile red, oxazine 725, and MBBA

In this work, the steady-state and time-resolved fluorescence anisotropies of nile red and oxazine 725 dissolved in the isotropic phase of *p*-methoxybenzylidene-*n*-butylaniline (MBBA) are measured, which give insight into the orientational dynamics of the dye molecules in the microscopically anisotropic liquid. Molecular structures of nile red, oxazine 725, and MBBA are shown in Figure 1. Nile red and oxazine 725 have been widely used as a fluorescent probe to investigate the reorientation dynamics in various solvents,[1−5,14,20] and the photophysics of these molecules has been studied as well.[21−24]

MBBA, which is one of the synthetic liquid crystalline materials with the longest historic background, crystallizes around 22 °C and exhibits the nematic phase between 22 and 47 °C. Only the nematic phase is observed for MBBA. The microscopic local order of the isotropic phase is related to the correlation length of the pseudonematic domain, ξ. The temperature dependence of the correlation length is given by[17]

$$\xi = \xi_0[T^*/(T - T^*)]^{1/2} \quad (4)$$

where ξ_0 is on the order of the molecular length and T^* is the same temperature as in eq 3. Below T_{NI}, the correlation length becomes infinite. Just above the phase transition temperature, the correlation length is of the order of $20\xi_0$ and decreases with the temperature rise. $3\xi_0$ is the minimum correlation length for which the LdG model applies. The transition to a simple liquid following the DSE equation occurs over a wide temperature range. ξ_0 for MBBA was measured to be in the range 5.5−7 Å,[25] and T^* for MBBA was found to be 46.4 °C. For MBBA, there are about 27 molecules within $3\xi_o$, and the temperature for $\xi = 3\xi_0$ is around 82 °C. In this work, the orientational dynamics of the dopant molecules in the isotropic MBBA have been studied in the temperature range where the LdG model is valid for neat MBBA.

Experimental Section

Nile red (Aldrich), oxazine 725 (perchlorate salt, Aldrich), and MBBA (Tokyo Kassei) were used as received. Absorption and emission spectra of nile red and oxazine 725 in several solvents were found to be consistent with the reported spectra.[14,22,23] The nematic−isotropic transition temperature of MBBA was not affected by the doping of dye molecules at the concentration of 5×10^{-5} M, which indicates that the dopant molecules give negligible effects on the properties of the host liquid crystal. All fluorescence anisotropy experiments were performed with the dye concentrations below 5×10^{-5} M where the concentration effect of the energy transfer or reabsorption on the fluorescence depolarization and emission spectra can be avoided. The absorption and fluorescence spectra were recorded by using a UV/vis absorption spectrophotometer (Varian, Cary 3) and a spectrofluorometer (Spex, FluoreMAX). The steady-state fluorescence anisotropy was measured in the L-format[26] and was found to be constant around the emission maxima (±10 nm) for nile red and oxazine 725.

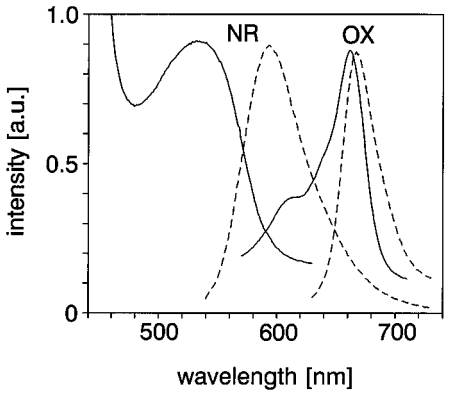

Figure 2. Absorption (solid lines) and emission (dashed lines) of nile red (NR) and oxazine 725 (OX) in the isotropic MBBA (50 °C). The excitation wavelengths for the emission spectra of nile red and oxazine 725 are 520 and 590 nm, respectively.

The time-resolved fluorescence decay was measured by using a time-correlated single photon counting (TCSPC) technique. A duel-jet dye laser (Coherent, 702-1) synchronously pumped by a mode-locked Ar^+ ion laser (Coherent, Innova 200) was used as an excitation source, and the fluorescence signal was detected by an MCP photomultiplier tube (Hamamatsu 2809U). The standard electronics were used for the TCSPC signal processing. The details of the experimental setup were previously reported.[27] The excitation wavelength for the time-resolved fluorescence measurement was 584 nm for nile red and 595 nm for oxazine 725. The emission was collected at 615 nm for nile red and 667 nm for oxazine 725. The emission signals of different polarization were separately detected by rotating the polarizer. The decay characteristics of the total fluorescence intensity were ascertained at the magic angle polarization condition. The time-resolved fluorescence anisotropies were determined from the separately deconvolved fluorescence components. The *G* factor was found to be one when the half-wave plate was placed in front of the detection system. The sample temperature was controlled within ±0.5 °C in a brass block using a water bath.

Results and Discussion

A. Steady-State Fluorescence. The absorption and fluorescence spectra of nile red and oxazine 725 in the isotropic MBBA at 50 °C are shown in Figure 2. Meanwhile, the absorption and emission profile of oxazine is not symmetric due to weak emission at the long wavelength; the emission profiles symmetric to the absorption profile are observed in other solvents. The spectral profile of the mirror image indicates that the absorption spectrum of oxazine in Figure 2 is due to a single electronic state. The large Stokes shift of nile red is attributed to the fluorescent twisted intramolecular charge transfer (TICT) state.[22] Molecules with flexible alkylamino groups are known to have the TICT state in polar solvents.[21−24] For oxazine derivatives[23,24] and aminophthalimide derivatives,[28] the TICT state is mostly nonfluorescent due to fast internal conversion. While the fluorescence from the TICT state is observed for nile red, the fluorescence from the planar excited state is observed for oxazine 725.

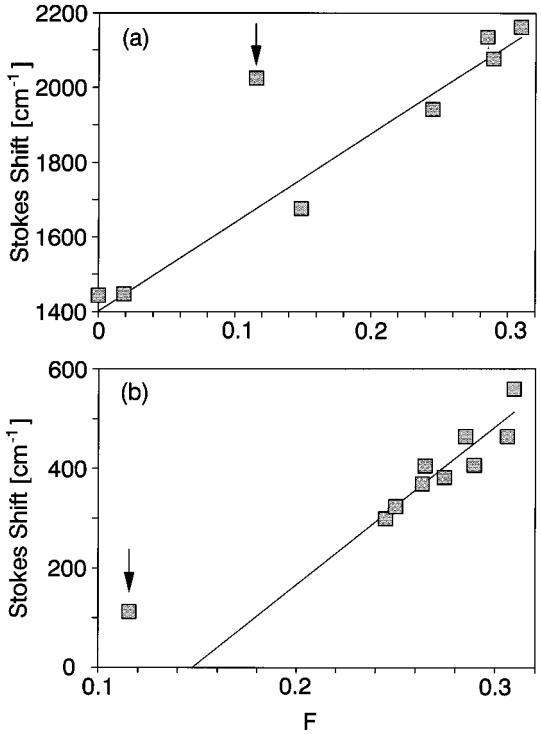

Figure 3. Steady-state Stokes shift vs F value for (a) nile red and (b) oxazine 725 in various solvents. The data points below the arrow correspond to the data points for MBBA. The ionic dye oxazine 725 is not dissolved in nonpolar solvents such as hexane or carbon tetrachloride, of which the F value is close to zero.

Figure 3 shows the Stokes shift of nile red and oxazine 725 in MBBA and other solvents. The Stokes shift ($\bar{\nu}_{abs} - \bar{\nu}_{em}$) of a solute molecule depends on the dielectric constant (ϵ) and the refractive index (n) of the solvent and is usually explained by the Lippert−Mataga equation[26]

$$\bar{\nu}_{abs} - \bar{\nu}_{em} = [2(\Delta\mu)^2/cha^3][(\epsilon - 1)/(2\epsilon + 1) - (n^2 - 1)/(2n^2 + 1)] + \text{constant} \quad (5)$$

where a is the cavity radius of the solute molecule and $\Delta\mu$ is the dipole moment difference of the excited and ground state of the solute molecule. According to the Lippert−Mataga equation, the Stokes shift of a dye molecule in various solvents is linear to $F = [(\epsilon - 1)/(2\epsilon + 1) - (n^2 - 1)/(2n^2 + 1)]$, and the slope is proportional to the square of the dipole moment change, $\Delta\mu$. The absorption and emission maxima in solvents other than MBBA agree with the reported values.[14,22,24]

The lines of Figure 3 are the linear regression results without including the data measured in MBBA. The dipole moment changes are estimated to be 5.5 ± 0.4 D for nile red and 4.7 ± 0.5 D for oxazine 725 from the slope. The previously used cavity radii of nile red (5.0 Å[1]) and oxazine 725 (4.1 Å[14]) are employed. The reported values of the dipole moment change are scattered in the range of 6−18 D for nile red[1−4,29,30] and estimated to be 4.5−5.5 D for oxazine 725.[14] We have no intention of quantitatively discussing the dipole moment of the fluorescent states of the dye molecules. However, it is noted that the Stokes shifts of the dye molecules in MBBA exhibit large positive deviation from the Lippert−Mataga relation. The Stokes shifts of the dye molecules in MBBA are greater than expected from the Lippert−Mataga equation, which suggests that the microscopic environment for the dye molecules in the isotropic MBBA may be more polar than deduced from the bulk properties of MBBA. If the anisotropy of the pseudonematic domains of the isotropic liquid crystals is effective for the dye molecules, the microscopic polarity would be greater than the bulk polarity. However, other experimental results discussed in the following sections show that the pseudonematic domains do not affect the fluorescence of the dye molecules. The Stokes shift in MBBA is considered to result from the relative sizes of MBBA and the dye molecules. As shown in Figure 1, the molecular size of MBBA is similar to the dye molecules so that the number of MBBA molecules surrounding the dye molecules is not so large as in the solution of small solvent molecules such as methanol. Therefore, the continuum model of solvation, on which the Lippert−Mataga equation is based, is not applicable for MBBA solution. The large molecular polarizability of MBBA[31] is not averaged for the dye molecule and causes the positive deviation of the Stokes shift in MBBA.

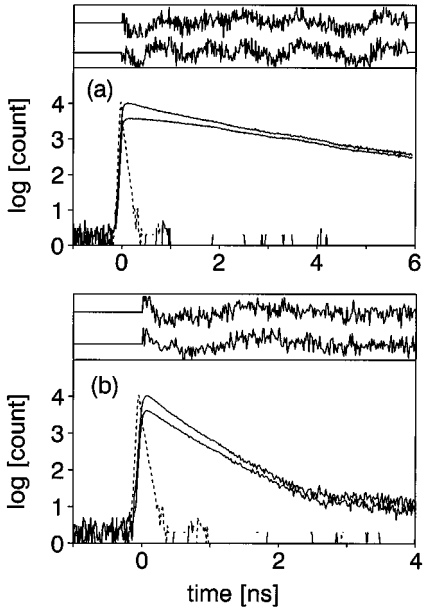

Figure 4. Typical fluorescence decay profiles for (a) nile red and (b) oxazine 725. The parallel (top curve) and perpendicular (bottom curve) component are shown with the instrument response function (dashed curve). The plots of residuals (scale = ±3.0) are given.

TABLE 1: Fluorescence Data of Nile Red in the Isotropic MBBA

			fluorescence anisotropy		
T (°C)	τ_f (ns)	τ_r (ns)	$r(0)$	r_{cal}[a]	r_{exp}
50	3.65	2.07	0.34	0.12	0.13
57	3.48	1.72	0.34	0.11	0.13
60	3.59	1.60	0.34	0.10	0.11
66	3.55	1.26	0.33	0.09	0.10
70	3.50	0.99	0.30	0.07	0.09
76	3.45	0.86	0.30	0.06	0.09
80	3.37	0.78	0.30	0.06	0.08

[a] Calculated by using eq 6.

B. Time-Resolved Fluorescence. Figure 4 shows typical temporal profiles of fluorescence decay for nile red and oxazine 725 in the isotropic MBBA. Nile red is excited at the wavelength of 584 nm in order to avoid complex dynamics involved with the formation of the planar nile red. As mentioned in the previous section, the fluorescent state of nile red is the TICT state and that of oxazine 725 is the planar state. Single-exponential decays for both total fluorescence intensity [$I = I_{\parallel} + 2I_{\perp}$] and anisotropy are observed for nile red. The fluorescence data for nile red and oxazine 725 in MBBA in the temperature range 50−80 °C are given in Tables 1 and 2, respectively. The χ^2 values of all data are between 1.1 and 1.4. The transition of nile red from the excited singlet state to

TABLE 2: Fluorescence Data of Oxazine 725 in the Isotropic MBBA

	fluorescence time constant (ns)			decay amplitude				fluorescence anisotropy		
T (°C)	τ_{rise}	τ_{decay1}	τ_{decay2}	A_{decay1}	A_{decay2}	$\tau_f{}^a$ (ns) ($\Sigma A_i\tau_i$)	$\tau_r{}^b$ (ns)	$r(0)$	$r_{cal}{}^c$	r_{exp}
50	0.08	0.30	0.81	0.72	0.28	0.44	1.99	0.33	0.27	0.30
56	0.07	0.27	0.70	0.72	0.28	0.39	1.49	0.34	0.27	0.29
60	0.06	0.26	0.65	0.74	0.26	0.36	1.28	0.34	0.27	0.28
66	<0.05	0.28	0.67	0.82	0.18	0.35	1.02	0.32	0.24	0.28
70	<0.05	0.26	0.64	0.87	0.13	0.31	0.97	0.35	0.27	0.28
76	<0.05	0.24	0.70	0.93	0.07	0.27	0.80	0.31	0.23	0.28
80	<0.05	0.22	0.71	0.96	0.04	0.24	0.98	0.34	0.27	0.28

[a] Fluorescence lifetime (average of two decay components). [b] Reorientation time. [c] Calculated by using eq 6.

the fluorescence TICT state is so fast that the rise of the fluorescence intensity is not observed.[22,30]

The fluorescence anisotropy of oxazine 725 decays single exponentially, but the total fluorescence intensity decays biexponentially. The fluorescence decay of oxazine 725 is sensitive to the solvent,[32] and the biexponential decay of total fluorescence intensity has been observed for oxazine derivatives in polar solvents.[21] Several interpretations are possible for the fluorescence characteristics of oxazine 725 in MBBA. An ionic molecule, a neutral complex with the counteranion, or molecules placed in inhomogeneous sites of the medium might reveal the same reorientation time but different fluorescence decay time. However, the emission spectra of mirror-image symmetry in other solvents indicate that the absorption spectra are not due to the neutral complex. While the fluorescence of oxazine 725 in glycerol decays single exponentially with the time constant of 2.0 ns,[32c] the biexponential decay with the overall decay time of ~0.6 ns is observed in methanol. These results support that reversible intramolecular transition between the emitting state and the TICT state may be responsible for the fluorescence dynamics of oxazine 725. The transition is inhibited in the viscous medium, but the interconversion between the emitting and nonemitting states is active in methanol, and nonradiative decay from the nonemitting state reduces the fluorescence decay time. Similar schemes are proposed for oxazine derivatives.[21] The temperature dependence of the relative amplitudes of two decay components given in Table 2 supports that intramolecular transition is relevant to the observed dynamics. That is, the fluorescence anisotropy of oxazine 725 results from the rotational relaxation in a mixture of the emitting and nonemitting states, and the dipole orientations are considered to be similar for these states.

While the fluorescence lifetime longer than the reorientation time is observed for nile red, the fluorescence lifetime shorter than the reorientation time is observed for oxazine 725 as given in Tables 1 and 2. The Perrin equation[26] gives the relation among these time constants, the steady-state fluorescence anisotropy r, and the intrinsic fluorescence anisotropy $r(0)$ as follows,

$$r = r(0)/[\tau_f/\tau_r + 1] \qquad (6)$$

where τ_f and τ_r are the fluorescence lifetime and reorientation time, respectively. The intrinsic anisotropy, corresponding to the anisotropy at $t = 0$, is related to the angle between the absorption and emission dipole moment, α, that is, $r(0) = (2/5)[(3\cos^2\alpha - 1)/2]$. When $r(0) = 0.34$, the angle α is about 18°. In the anisotropic medium of aligned rod-shaped molecules such as MBBA, the steady-state anisotropy is greater than estimated by the Perrin equation.[33,34] A good agreement of the measured steady-state anisotropies with the Perrin equation suggests that the MBBA medium for the dye molecules is isotropic.

The fluorescence lifetime of nile red is sometimes used as a criterion for the polarity of the medium.[22,35] The activation energy barrier for the nonradiative processes from the TICT state to the triplet state decreases in polar solvents, and the fluorescence decay time constant decreases with the increase of solvent polarity. Although MBBA ($\epsilon = 5.2$)[36] is not so polar as ethanol ($\epsilon = 24.3$) or methanol ($\epsilon = 33.7$),[37] the fluorescence lifetime of nile red in the isotropic MBBA (3.65 ns at 50 °C) is similar to that in ethanol (3.6 ns at 25 °C) and methanol (3.6 ns at 25 °C).[22] The fluorescence lifetimes of nile red are observed to be 5.1 ns in CCl_4 ($\epsilon = 2.2$) and 4.3 ns in $CHCl_3$ ($\epsilon = 4.8$).[22] The short fluorescence lifetime of nile red in MBBA is attributable to high polarizability of MBBA as the Stokes shift of the dye molecules in the isotropic MBBA deviates from the Lippert−Mataga equation. The relatively short fluorescence lifetime of nile red in the isotropic MBBA, which results from the reduced activation barrier for the conversion from the TICT state to triplet state, is ascribed to the molecular property of MBBA rather than the property due to the local structure of the isotropic phase of MBBA. The fluorescence characteristics of the dye molecule including the good agreement with the Perrin equation indicate that the dopant dye molecules are not coupled with the local structure of the microscopic anisotropy of the isotropic MBBA.

C. Orientational Dynamics. The orientation times of nile red and oxazine 725 in the isotropic MBBA are plotted as a function of viscosity/temperature in Figure 5. The reported viscosity values for the isotropic MBBA[38] are used. The lines of Figure 5 represent the reorientation time estimated from the DSE model of eq 2 for the stick boundary condition. The van der Waals volumes of nile red[1,2] and oxazine 725[14] are 285 and 294 Å^3, respectively. To estimate the molecular shape factor for nile red and oxazine 725, the following molecular parameters are used: the molecular axes are 8.4 Å:4.7 Å:2.5 Å for nile red[1,2] and 9.2 Å:4.6 Å:2.5 Å for oxazine 725.[14,39] The molecular shape factors (f) are calculated as 1.4 for nile red and 1.5 for oxazine 725 using the expression for the prolate molecule.[40] The reorientation times of nile red and oxazine 725 in the isotropic MBBA are close to the estimation of the DSE model but much smaller than that of the LdG model. The orientational time by the LdG model of eq 3 is about 300 times greater than the reorientation time by the DSE model at 47 °C ($\eta/T = 0.057$) and 10 times greater at 80 °C ($\eta/T = 0.017$).

Failure of the LdG model and absence of the fast component by the intradomain relaxation for the orientational dynamics of the dye molecules in the isotropic MBBA indicate that the rotation of the dopant dye molecules is not affected by the local structures of the isotropic liquid crystal. Dynamics of the fast intradomain relaxation follow a temperature-independent power law of $t^{-0.63}$, which is universal behavior in the isotropic liquid crystals on ultrafast time scales and short distance scales.[41] For the neat isotropic MBBA, the intradomain relaxation was observed over the first 1 ns in the temperature range investigated

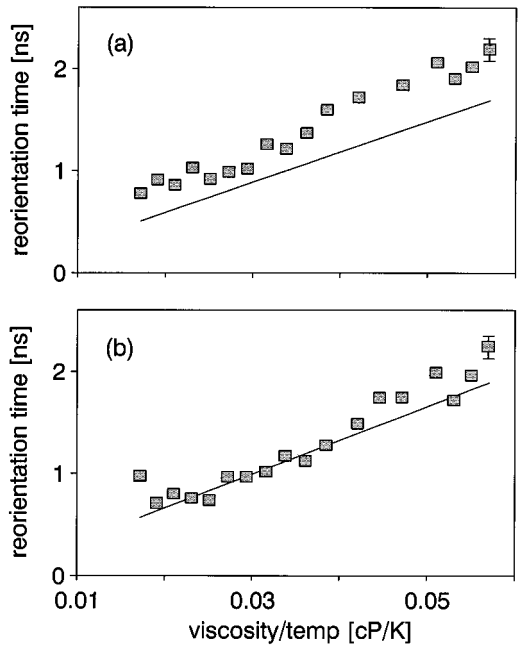

Figure 5. Viscosity/temperature dependence of the reorientation time for (a) nile red and (b) oxazine 725 in MBBA. The line represents the reorientation time by DSE model in the stick boundary condition.

in this work.[18] The power law exhibits the signal change much faster than the exponential decay on the nanosecond time scale. The absence of the intradomain relaxation implies that the dye molecules are not coupled with the pseudonematic domains. The dye molecules are considered to be placed between the randomly oriented pseudonematic domains. Therefore, the microscopic anisotropy of the isotropic MBBA does not affect the reorientation dynamics of the dopant dye molecules. The affinity between the MBBA molecules in the pseudonematic domain is stronger than the affinity between the dye molecule and the MBBA molecule. The results are consistent with the validity of the DSE model and the Perrin equation, which indicates that the environment for the dye molecules is isotropic in the isotropic MBBA.

The small positive deviation of the reorientation times from the DSE model of Figure 5 is usually explained in terms of the dielectric friction.[1−4,11,14,15] The rotation of polar molecules induces the polarization in the surrounding solvent medium, and the lag of the induced polarization around the solute molecule causes the dielectric friction, which results in an increase of the reorientation time of the solute. When the dielectric friction is included in the reorientation dynamics, the reorientation time τ_{reo} is expressed by a sum of the reorientation times due to the hydrodynamic and the dielectric friction.

$$\begin{aligned}\tau_{reo} &= \tau_{DSE} + \tau_{DF} \\ &= \eta Vf/kT + (\mu^2/a^3kT)g(\epsilon,\tau_D) \\ &= (1/6kT)\zeta \\ &= (1/6kT)(\zeta_{DSE} + \zeta_{DF}) \end{aligned} \quad (7)$$

where μ is the dipole moment of the rotating molecule, τ_D is the Debye dielectric relaxation time of solvent, and ζ's represent corresponding frictions. The other parameters are the same as those in eqs 2 and 5. The detailed form of the function $g(\epsilon,\tau_D)$ depends on the models for the dielectric friction. Generally, the dielectric friction decreases with the increase of the dielectric constant of the solvent and increases with the dielectric relaxation time of the solvent which is proportional to (η/T). However, it is not easy to make a quantitative estimation of the dielectric friction since the involved parameters cannot be determined accurately: the dipole moment of the excited state, the temperature dependence of the dielectric relaxation time usually measured by time domain reflectometry techniques,[42] and the rotation cavity radius calculated based on the van der Waals volume of the rotating molecule should be known.

Among various models for the dielectric friction, the model by van der Zwan and Hynes[43] exhibits a good agreement with the experimental observations for oxazine 725.[14] The contribution of the dielectric friction ζ_{DF}/ζ for the excited state of oxazine 725 was estimated to be 15−20% in several alcohols. The fractions of the dielectric friction ζ_{DF}/ζ for nile red and oxazine 725 can be calculated from the data shown in Figure 5. The average fraction of the dielectric friction in the isotropic MBBA is 30 ± 6% for nile red and 15 ± 10% for oxazine 725. The fraction of the dielectric friction for oxazine 725 is consistent with the reported values. The greater fraction of the dielectric friction for nile red is due to the larger dipole moment of the excited state of nile red. The dipole moment of the ground-state nile red is reported to be 7 D.[29] The dipole moment of the excited-state nile red is estimated to be about 12 D from the dipole moment change by the Lippert−Mataga equation; meanwhile, the dipole moment of the excited-state oxazine 725 is deduced to be 6.2 D.[14] The contribution of the dielectric friction, which is consistent with the reported value, indicates that the hydrodynamic model with the dielectric friction is appropriate for the orientational dynamics of the dopant molecules in the isotropic MBBA. The microscopic anisotropy of the isotropic liquid crystal, which influences strongly the orientational dynamics of neat liquid crystals, does not affect the rotation of the dopant dye molecules.

Summary

Nile red and oxazine 725 are used as the fluorescence probe for the study of the microscopic structure of the isotropic MBBA. The steady-state and time-resolved fluorescence anisotropy of the probe molecules can be interpreted by the hydrodynamic models such as the Perrin equation, the Debye−Stokes−Einstein model, and the dielectric friction. The microscopic anisotropy of the pseudonematic domain of the isotropic liquid crystal, which is important in the Landau−de Gennes model for the dynamics of neat isotropic liquid crystals, does not affect the orientational dynamics of the dopant dye molecules in the isotropic MBBA. Intermolecular association of MBBA molecules are considered to be so strong that the insertion of dopant molecules into pseudonematic domains is not allowed, and the dopant molecules feel the averaged field by the motions of the pseudonematic domains in the isotropic phase of the liquid crystal.

Acknowledgment. This work is supported by grants from the Ministry of Education of Korea (BSRI-96-3432) and the Korean Science and Engineering Foundation (94-1400-02-01-3). T.J.K. was supported in part by the Taegu University research grant (1997), and D.K. was supported by the Center for Molecular Science through KOSEF.

References and Notes

(1) Dutt, G. B.; Doraiswamy, S.; Periasamy, N.; Venkataraman, B. *J. Chem. Phys.* **1990**, *93*, 8498.

(2) Dutt, G. B.; Doraiswamy, S.; Periasamy, N. *J. Chem. Phys.* **1991**, *94*, 5360.

(3) Dutt, G. B.; Doraiswamy, S. *J. Chem. Phys.* **1992**, *96*, 2457.

(4) Krishnamurty, M.; Khan, K. K.; Doraiswamy, S. *J. Chem. Phys*. **1993**, *98*, 8640.
(5) Williams, A. M.; Jiang, Y.; Ben-Amotz, D. *Chem. Phys*. **1994**, *180*, 119.
(6) Rasimas, J. P.; Blachard, G. J. *J. Phys. Chem*. **1995**, *99*, 11333.
(7) Levitus, M.; Negri, R. M.; Aramendia, P. F. *J. Phys. Chem*. **1995**, *99*, 14231.
(8) Imeshev, G.; Khundkar, L. R. *J. Chem. Phys*. **1995**, *103*, 8322.
(9) Heitz, M. P.; Bright, F. V. *J. Phys. Chem*. **1995**, *100*, 6889.
(10) Backer, S. D.; Dutt, G. B.; Ameloot, M.; Schryver, F. C. D.; Mullen, K.; Holtrup, F. *J. Phys. Chem*. **1996**, *100*, 512.
(11) Horng, M.-L.; Gardecki, J. A.; Maroncelli, M. *J. Phys. Chem. A* **1997**, *101*, 1030.
(12) Dorfmuller T., Pecora, R., Eds. *Rotational Dynamics of Small and Macromolecules*; Springer: Berlin, 1987.
(13) Hu, C.-M.; Zwanzig, R. *J. Chem. Phys*. **1974**, *60*, 4354.
(14) Simon J. D.; Thompson, P. A. *J. Chem. Phys*. **1990**, *92*, 2891.
(15) (a) Hartman, R. S.; Waldeck, D. H. *J. Phys. Chem*. **1994**, *98*, 1386. (b) Papazyan, A.; Maroncelli, M. *J. Chem. Phys*. **1995**, *102*, 2888. (c) Srivastava, A.; Doraiswamy, S. *J. Chem. Phys*. **1995**, *103*, 6197.
(16) (a) Stein, A. D.; Fayer, M. D. *J. Chem. Phys*. **1992**, *97*, 2948. (b) Alvai, D. S.; Hartman, R. S.; Waldeck, D. H. *J. Chem. Phys*. **1991**, *95*, 6770.
(17) de Gennes, P. G. *The Physics of Liquid Crystals*; Clarendon: Oxford, 1974.
(18) (a) Stankus, J. J.; Torre, R.; Marshall, C. D.; Greenfield, S. R.; Sengupta, A.; Tokmakoff, A.; Fayer, M. D. *Chem. Phys. Lett*. **1992**, *194*, 213. (b) Stankus, J. J.; Torre, R.; Fayer, M. D. *J. Phys. Chem*. **1993**, *97*, 9478.
(19) Deeg, F. W.; Greenfield, S. R.; Stankus, J. J.; Newell, V. J.; Fayer, M. D. *J. Chem. Phys*. **1990**, *93*, 3503.
(20) Blanchard, G. J. *J. Phys. Chem*. **1988**, *92*, 6303.
(21) Vogel, M.; Rettig, W.; Fiedeldei, U.; Baumgartel, H. *Chem. Phys. Lett*. **1988**, *148*, 347.
(22) Dutta, A. K.; Kamada, K.; Ohta, K. *J. Photochem. Photobiol. A* **1996**, *93*, 57.
(23) Rettig, W.; Vogel, M.; Lippert, E.; Otto, H. *Chem. Phys*. **1986**, *103*, 381.
(24) Vogel, M.; Rettig, W. *Ber. Bunsen-Ges. Phys. Chem*. **1985**, *89*, 962.
(25) (a) Chu, B.; Bak, C. S.; Lin, F. L. *Phys. Rev. Lett*. **1972**, *28*, 1111. (b) Courtens, E.; Koren, G. *Phys. Rev. Lett*. **1975**, *35*, 1711. (c) Gulari, E.; Chu, B. *J. Chem. Phys.* **1975**, *65*, 798. (d) Courtens, E. *J. Chem. Phys*. **1977**, *66*, 3995.
(26) Lakowicz, J. R. *Principles of Fluorescence Spectroscopy*; Plenum: New York, 1983.
(27) Yang, S. I.; Suh, Y. D.; Jin, S. M.; Kim, S. K.; Park, J.; Shin, E. J.; Kim, D. *J. Phys. Chem*. **1996**, *100*, 9223.
(28) Soujanya, T.; Fessenden, R. W.; Samanta, A. *J. Phys. Chem*. **1996**, *100*, 3507.
(29) Reiser, D.; Laubereau, A. *Ber. Bunsen-Ges. Phys. Chem*. **1982**, *86*, 1106.
(30) Sarkar, N.; Das, K.; Nath, D. N.; Bhattacharyya, K. *Langmuir* **1994**, *10*, 326.
(31) Khoo, I.-C.; Wu, S.-T. *Optics and Nonlinear Optics of Liquid Crystals*; World Scientific: Singapore, 1993.
(32) (a) Morgenthaler, M.; Meech, S. R.; Yoshihara, K. *Chem. Phys. Lett*. **1992**, *197*, 537. (b) Nagasawa, Y.; Yartsev, A. P.; Tominaga, K.; Johnson, A. E.; Yoshihara, K. *J. Chem. Phys*. **1994**, *101*, 5717. (c) Morgenthaler, M.; Yoshihara, K. Meech, S. R. *J. Chem. Soc., Faraday. Trans.* **1996**, *92*, 629.
(33) Szabo, A. *J. Chem. Phys*. **1980**, *72*, 4620.
(34) Chapoy, L. L.; Dupre, D. B. *J. Chem. Phys*. **1978**, *69*, 519.
(35) Dutta, A. K.; Kamada, K.; Ohta, K. *Chem. Phys. Lett*. **1996**, *258*, 369.
(36) (a) Blinov, L. M. *Electro-optical and Magneto-optical Properties of Liquid Crystals*; Wiley: New York; 1983. (b) Chandrasekhar, S. *Liquid Crystals*, 2nd ed.; Cambridge: New York, 1992.
(37) Lide, D. R., Ed. *CRC Handbook of Chemistry and Physics*, 75th ed.; CRC: Boca Raton, FL, 1994.
(38) Martinoty, P.; Candau, S.; Debeauvais, F. *Phys. Rev. Lett*. **1971**, *27*, 1123.
(39) (a) Edward, J. T. *J. Chem. Educ*. **1970**, *47*, 261. (b) Bondi, A. *J. Phys. Chem*. **1964**, *68*, 441.
(40) Fleming, G. R. *Chemical Applications of Ultrafast Spectroscopy*; Oxford: New York, 1986.
(41) Sengupta, A.; Fayer, M. D. *J. Chem. Phys*. **1995**, *102*, 4193.
(42) (a) Kumbharkhane, A. C.; Puranik, S. M.; Mehrotra, S. C. *J. Chem. Soc., Faraday Trans*. **1991**, *87*, 1569. (b) Cile, R. H.; Berberian, J. G.; Mashimo, S.; Chryssikos, G.; Burns, A. *J. Appl. Phys*. **1989**, *66*, 793.
(43) van der Zwan, G.; Hynes, J. T. *J. Phys. Chem.* **1985**, *89*, 4181.